Journal of Sound and Vibration (1999) **226**(4), 799–805
Article No. jsvi.1999.2288, available online at http://www.idealibrary.com on IDEAL®

COMMENTS ON "A FREQUENCY DOMAIN BASED NUMERIC-ANALYTICAL METHOD FOR NON-LINEAR DYNAMICAL SYSTEMS"

R. VAN DOOREN

Department of Mechanical Engineering, Free University of Brussels, Pleinlaan 2, *B*-1050 *Brussels, Belgium*

(*Received* 19 *March* 1999)

The authors S. Narayanan and P. Sekar are to be congratulated with their very interesting paper [1] on a multi-harmonic balance technique for determining periodic orbits in non-linear dynamical systems. It is important that the method can deal with all types of excitations and non-linearities and that it can also treat higher-dimensional systems. In this method the non-linear differential equations are transformed into a non-linear system of algebraic equations in terms of the Fourier coefficients of the periodic solutions. The so-called Fourier–Galerkin–Newton method is established such that algorithms based on the fast Fourier transform and on the discrete Fourier transform can be applied. The transitions from stable to unstable periodic orbits are studied by the use of the Floquet theory. The continuation of a particular solution branch is performed through a predictor–corrector method. A cubic extrapolation procedure is applied for prediction and a least-squares minimization in conjunction with singular value decomposition is used for correction. The efficiency of the method has been illustrated with two examples on impact and contact vibrations.

I should like to make two comments on their paper. The first comment is concerned with example 1 on the impacting non-linear oscillator governed by the differential equation

$$\ddot{x} + 2\zeta\dot{x} + x + g(x, \dot{x}) = P\cos(\omega t), \tag{1}$$

with

$$g(x, \dot{x}) = \begin{cases} C_H(x-\delta)^{3/2}(1+\beta\dot{x}) & \text{for } x > \delta \\ 0 & \text{for } x \leqslant \delta, \end{cases} \tag{2}$$

where ζ is the linear damping coefficient, C_H is the Hertzian constant, β is the hysteretic damping parameter, P and ω are the amplitude and the frequency of the periodic excitation. The dots represent differentiation with respect to time t. The

0022-460X/99/390799 + 07 $30.00/0

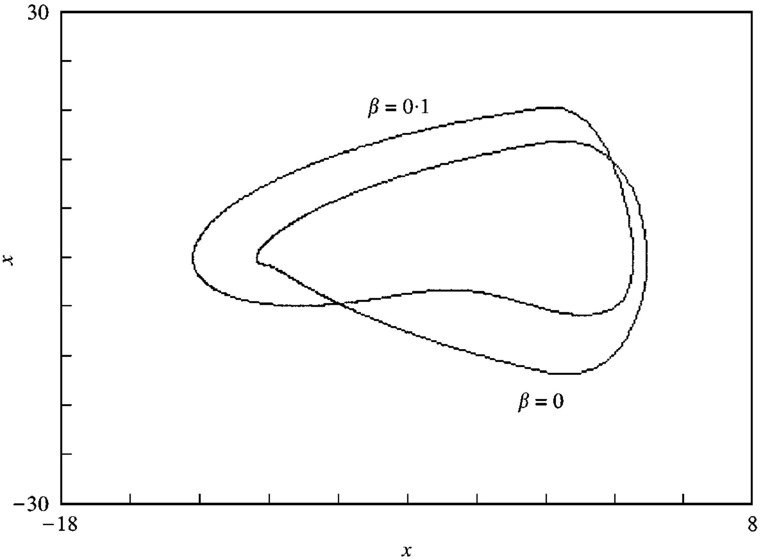

Figure 1. Phase plane plot showing the cases $\beta = 0{\cdot}0$ and $0{\cdot}1$ for example 1 ($\zeta = 0{\cdot}05$, $C_H = 10{\cdot}0$, $\delta = 0{\cdot}0$, $P = 10{\cdot}0$, $\omega = 1{\cdot}2$).

parameters mentioned in reference [1] in the caption of Figure 1 and in the line just preceding this figure are: $\zeta = 0{\cdot}05$, $\beta = 0{\cdot}0$, $C_H = 10{\cdot}0$, $\delta = 0{\cdot}0$, $P = 10{\cdot}0$, $\omega = 1{\cdot}2$. It has been pointed out that the mentioned value of $\beta = 0{\cdot}0$ is not the correct one. The plot of the orbit in the phase plane for the case $\beta = 0{\cdot}0$ is as given in Figure 1 of this Letter. Numerical experiments with several values of β have been considered. This reveals that the phase portrait in Figure 1 from reference [1] (the curve indicated by the digits 5, 6, 7, 8 for iterations and the abbreviation NI for applying the numerical integration method) corresponds to the case $\beta = 0{\cdot}1$. For comparison both cases $\beta = 0{\cdot}0$ and $0{\cdot}1$ have been represented in Figure 1 of this Letter.

The second comment applies to example 2 on the vibrations of two elastic bodies in rolling contact, one with a smooth surface and the other with a wavy surface. The contact is assumed to be Hertzian. The equation of contact vibration can be written as [1]

$$\ddot{x} + 2\zeta\dot{x} + (2/3)[\mathrm{H}(x)x^{3/2} - 1] = -\xi_0\Omega[\Omega\cos(\Omega t) + 2\zeta\sin(\Omega t)], \tag{3}$$

where $\mathrm{H}(x)$ is the Heaviside unit step function. Equation (3) has been solved in reference [1] by the Fourier–Galerkin–Newton method with the discrete Fourier transform in conjunction with the path following algorithm and the stability analysis according to the Floquet theory. Period -1, -2, -4 and -3 orbits have been found in the range of the frequency Ω varying from $0{\cdot}0$ to $3{\cdot}0$. However, the period -6 orbit in the vicinity of $\Omega = 1{\cdot}87$ with $\zeta = 0{\cdot}05$ and $\xi_0 = 0{\cdot}5$ has not been mentioned. For $\Omega = 1{\cdot}87$ one has the coexistence of period -3, -2 and 6 orbits as far as the stable orbits are concerned (unstable period-1 and -3 orbits also occur). Period -6 orbit is readily found by direct numerical integration of equation (3)

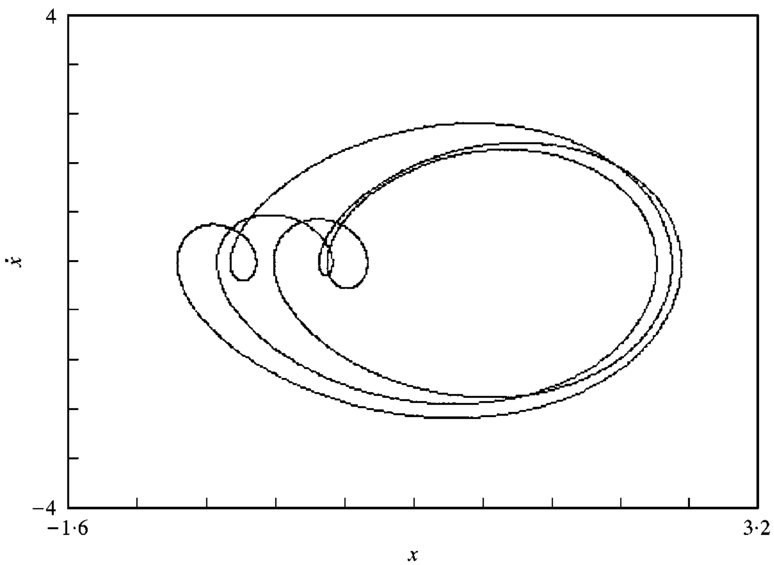

Figure 2. Phase plane plot of the period-6 orbit for example 2 ($\zeta = 0{\cdot}05$, $\xi_0 = 0{\cdot}5$, $\Omega = 1{\cdot}87$).

starting, e.g. from the initial point $x = 1$, $\dot{x} = 0$ in the phase plane (the so-called brute force method). The orbit is spiralling towards the limit cycle. This last one is represented in Figure 2. The co-ordinates $(x, \dot{x})$ of the Poincaré section points corresponding to $t = 0$ in the phase plane are found as follows:

period-3: $(-2{\cdot}9277, -0{\cdot}5727)$, $(-1{\cdot}1872, 1{\cdot}4932)$, $(3{\cdot}0977, -1{\cdot}8027)$;
period-2: $(2{\cdot}6234, -0{\cdot}4391)$, $(0{\cdot}0122, 0{\cdot}2069)$;
period-6: $(0{\cdot}4601, 0{\cdot}1826)$, $(2{\cdot}4450, -0{\cdot}5564)$, $(0{\cdot}1865, 0{\cdot}3238)$,
$(2{\cdot}5912, -0{\cdot}7294)$, $(-0{\cdot}3109, 0{\cdot}1742)$, $(2{\cdot}5967, -0{\cdot}0316)$.

The six Poincaré section points of the period-6 orbit occur in two clusters, each group of three points surrounding one of the Poincaré section points representing the period-2 orbit.

It is highly instructive to determine the basins of attraction of the period -3, -2 and -6 orbits. A grid of initial conditions in the relevant phase space is taken and time integrations of equation (3) are performed for each of these initial conditions. A different level of grey is assigned to each initial condition related to the distinct steady state attractor that the orbit approaches (see reference [2]). Figure 3 shows the basins of attraction for $\Omega = 1{\cdot}87$, $\zeta = 0{\cdot}05$ and $\xi_0 = 0{\cdot}5$ in the phase plane with $-4 \leqslant x \leqslant 4$ and $-4 \leqslant \dot{x} \leqslant 4$ and with resolution 200×200. This figure was obtained from Nusse and Yorke's package DYNAMICS [3]. The coherent black domain is the basin of the period-3 orbit. The basins of the period-2 and -6 orbits are intertwined. The dark grey region is the basin of attraction of the period-6 orbit and the light grey region corresponds to the period-2 orbit.

A careful study of the continuation of the period-6 orbit is needed. In the continuation technique based on the shooting method [4–6] equation (3) is

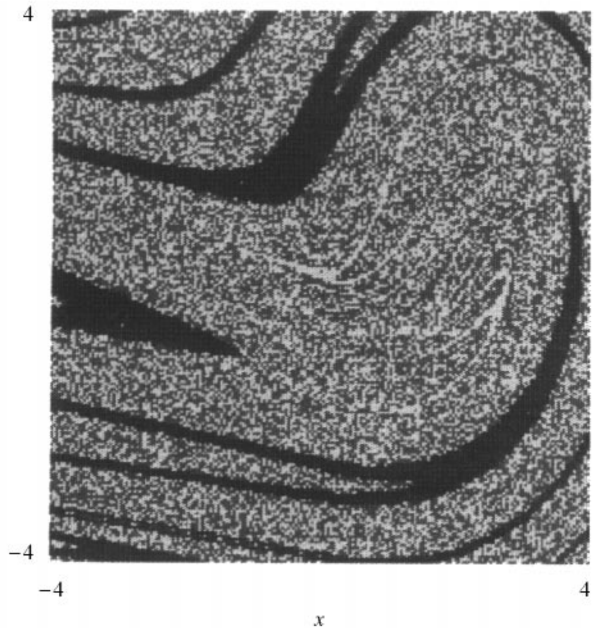

Figure 3. Basins of attraction for example 2 ($\zeta = 0{\cdot}05$, $\xi_0 = 0{\cdot}5$, $\Omega = 1{\cdot}87$). Coherent domain: period-3, in black. Intertwined domain: period-6, in dark grey; period-2, in light grey.

rewritten as

$$\dot{\mathbf{x}} = \mathbf{X}(\mathbf{x}, t), \tag{4}$$

in which $\mathbf{x}$ is two-dimensional. Chose $\mathbf{x}$ as the starting point of the procedure. One considers the system of the first variational equations derived from the original system (4) with respect to the reference solution $\mathbf{x}(t, \mathbf{x}_0)$ having the relevant period T:

$$\dot{\mathbf{z}} = \mathbf{X}_{\mathrm{x}}[\mathbf{x}(t, \mathbf{x}_0), t]\mathbf{z}, \tag{5}$$

where $\mathbf{X}_{\mathrm{x}}$ denotes the corresponding partial derivative. Let $\mathbf{\Phi}(t)$ be the fundamental matrix of the system of the first variational equations with initial condition $\mathbf{\Phi}(0) = \mathbf{I}$, $\mathbf{I}$ being the identity matrix. In the shooting method the starting point $\mathbf{x}_0$ is ameliorated in an iterative manner by determining the correction vector $\Delta\mathbf{x}_0 = \mathbf{x}_{\mathrm{new}} - \mathbf{x}_0$. This vector is the solution of the system of linear equations

$$[\mathbf{I} - \mathbf{\Phi}(T)]\Delta\mathbf{x}_0 = \mathbf{r}_0, \tag{6}$$

where $\mathbf{r}_0 = \mathbf{x}(T, \mathbf{x}_0) - \mathbf{x}_0$, i.e. the error at the end $t = T$ of the numerical integration of equation (4). The stability of the periodic orbit is investigated by applying the Floquet theory. Transitions from stable to unstable solutions occur when one of the eigenvalues of the matrix $\mathbf{\Phi}(T)$ crosses the unit circle in the complex plane.

The results of the continuation procedure taking small changes of the frequency parameter Ω are illustrated in Figure 4 which represents the amplitude of the

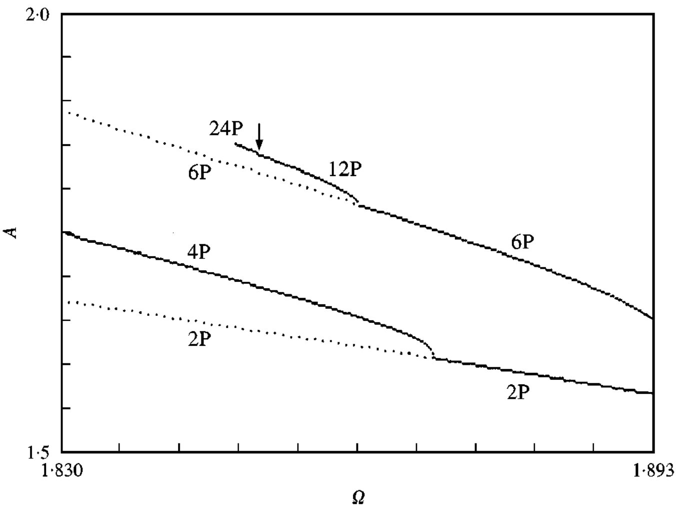

Figure 4. Response amplitude diagram of the period-2 and -6 orbits and their bifurcations in example 2 for $1{\cdot}830 \leqslant \Omega \leqslant 1{\cdot}893$ ($\zeta = 0{\cdot}05$, $\xi_0 = 0{\cdot}5$), —— stable; - - - -, unstable.

relevant vibration, defined as $A = (x_{max} - x_{min})/2$, in the frequency domain ranging from 1·830 to 1·893 with $\zeta = 0{\cdot}05$ and $\xi_0 = 0{\cdot}5$. The period-6 orbit appears at a value of Ω slightly below $\Omega = 1{\cdot}8933$ with one of the eigenvalues near to the value $+1$. If Ω is decreased the stable period-6 orbit loses stability at the transition value $\Omega = 1{\cdot}86156$ for which one of the eigenvalues passes through the value -1. At this value of Ω a bifurcation to a stable period-12 orbit takes place. The next transition from period-12 to period-24 occurs at $\Omega = 1{\cdot}85078$. The transition from period-24 to period-48 is found to occur at $\Omega = 1{\cdot}84845$. Note that the amplitudes of these periodic solutions fall within the amplitude range from 0·0 to 5·0 considered in Figure 5 in reference [1]. In Figure 4 of this Letter full lines indicate stable orbits and dotted lines represent unstable orbits. The arrow shows the transition point for the bifurcation from period-12 to period-24 orbit. The unstable branches for period-12 and -24 orbits have been omitted for clarity. The amplitudes of the period-2 and 4 orbits from Figure 5 in reference [1] have been redrawn in Figure 4. The amplitudes of the period-6, -12 and -24 orbits are higher than those of the period-2 and -4 orbits. It has been pointed out that the continuation of the left part of the period-6 solution remains unstable until at least $\Omega = 1{\cdot}6$.

In conclusion, since the basins of attraction of the period-2 and -6 orbits (or their bifurcated orbits) are intertwined, the existence and characteristics of the period-6 orbit and its bifurcations for equation (3) should be mentioned.

REFERENCES

1. S. Narayanan and P. Sekar 1998 *Journal of Sound and Vibration* **211**, 409–424. A frequency domain based numeric-analytical method for non-linear dynamical systems.
2. C. Pezeshki and E. H. Dowell 1987 *Journal of Sound and Vibration* **117**, 219–232. An examination of initial condition maps for the sinusoidally excited buckled beam modeled by the Duffing's equation.

3. H. E. Nusse and J. A. Yorke 1998 *Dynamics: Numerical Explorations.* New York; Springer, second edition.
4. P. Deuflhard 1984 *BIT* **24**, 456–466. Computation of periodic solutions of nonlinear ODE's.
5. R. Van Dooren and H. Janssen 1996 *Journal of Computational and Applied Mathematics* **66**, 527–541. A continuation algorithm for discovering new chaotic motions in forced Duffing systems.
6. R. Van Dooren 1996 *Chaos, Solitons and Fractals* **7**, 77–90. Chaos in a pendulum with forced horizontal support motion: a tutorial.

AUTHORS' REPLY

S. Narayanan and P. Sekar

Machine Dynamics Laboratory, Department of Applied Mechanics, Indian Institute of Technology Madras, Chennai 600 036, *India*

(*Received* 16 *April* 1999)

The authors wish to thank R. Van Dooren [1] for his interest in our paper [2] and for his general appreciation of the scheme of the numeric-analytical method presented in the paper for determining periodic orbits of non-linear dynamical systems which can treat different types of excitations and non-linearities and which can treat higher-dimensional systems.

As far as the comments of Van Dooren, we make the following observations.

The aim of the paper was to present a frequency domain based numeric-analytical method coupled with a stability analysis and path following approach. The efficacy of the iteration scheme was demonstrated in example 1 of reference [2] by showing how the successive iterations approach the accurate solution from the initial arbitarily chosen one. Example 2 was used to demonstrate the stability analysis and path following approach.

As has been pointed out by Van Dooren the value of β in the caption of Figure 1 of reference [2] as well as the line just preceding the figure should have been $\beta = 0.1$ and not $\beta = 0$. Since the problem was solved for many values of β, this error had inadvertantly crept in. We wish to thank Van Dooren for the correction.

The numeric-analytical algorithm presented in reference [2] was used to trace the response curve of example 2 starting from the point 'a' in Figure 5. The fold bifurcation points b and c and flip bifurcation points d and e were detected by stability analysis while the response curve was traced. Period-2 motion which bifurcated from the point e(flip) was further traced which goes along points f (flip), g (flip), h (fold) and ultimately merged with point d (flip-subcritical). Period-4 motion bifurcated from the point f was also traced which merged with point g. This exercise demonstrated the stability analysis and path following approach.

While determining the domains of attraction we discovered the presence of remote period-3 motion and then we traced its response curve [3]. However, we did